JOURNAL OF MATERIALS SCIENCE 29 (1994) 4786–4792

Processing conditions–fracture toughness relationships of asphalt concrete mixtures

H. AGLAN
Department of Mechanical Engineering, Tuskegee University, Tuskegee, AL 36088, USA
A. OTHMAN, L. FIGUEROA
Department of Civil Engineering, Case Western Reserve University, Cleveland, OH 44106, USA

The effect of processing conditions (dynamic compaction) on the fatigue crack propagation behaviour of AC-20 asphalt concrete mixture was studied. Beams were prepared from AC-20 asphalt binder containing 8% asphalt by weight with and without dynamic compaction. The gradation used was Ohio Department of Transportation item 403, and was kept the same. Flexural static tests were conducted to determine the effect of dynamic compaction on both the ultimate strength and flexural modulus. Flexural fatigue tests were conducted on three identical notched specimens prepared using each of the two compaction techniques. Parameters controlling the crack propagation process were evaluated; namely, the energy release rate and the change in work, $\dot{W}_i$ expended on damage formation and history dependent viscous dissipation processes within the active zone (region ahead of the crack tip). The modified crack layer (MCL) model was employed to extract the specific energy of damage, γ', a material parameter characteristic of the asphalt concrete mixture's resistance to crack propagation, and the dissipative coefficient, β'. It has been found that the dynamically and statically compacted AC-20 mixture displayed superior fracture resistance, as reflected in γ' and β'. Also, the ultimate strength and modulus increased by about two-fold. Scanning electron microscopic examination revealed an obvious change in the morphology of the fracture surface. This is manifested in the appearance of a finer more dense texture in the case of the dynamically and statically compacted mixture. In addition, smaller more frequent dimples in binder rich areas are indicative of better adhesion between the binder and the aggregate. This in turn contributes to the increased fracture resistance of the dynamically and statically compacted AC-20 asphalt concrete mixture.

1. Introduction

Increased traffic loading density, and high repetitive pressures resulting from heavy vehicles, are among the factors that cause cracking, leading to premature failure of pavements. Although extensive research has been done on various aspects of asphalt pavements, to reduce their susceptibility to cracking, studies of the effect of compaction on pavement performance have not been given as much attention. It has been widely recognized that the better the pavement compaction, the more uniform the density will be. Compacted specimens have shown a reduction in air void content, as well as a tremendous improvement in mechanical properties, such as strength and stiffness, material uniformity, surface finish, etc. The better the compaction, the better the resistance of asphalt pavements to wear, premature failure, deformation and induced stresses by heavy traffic [1, 2]. The payoff of these improved mechanical properties include reduced maintenance costs, limited periodic maintenance and reduced inconvenience to users.

The best laboratory compaction technique should be capable of producing pavement with engineering properties very close to those measured from field cores. The Marshall method of mix design, which is one of the most widely used methods, consists of compacting mix specimens, density–void analysis and testing for stability and flow (ASTM D1559). A variety of other laboratory compaction methods such as the California kneading compactor (AASHTOT247-80), Texas gyratory shear compactor (ASTM D4013-81), the mobile steel-wheel vibratory simulator, and the Arizona vibratory kneading compactor are being evaluated for potential use by agencies involved in asphalt concrete mixture design [3]. Any of these compaction methods, including the Marshall method, appear to be capable of ranking various pavements in a laboratory setup. For example, studying the effect of asphalt type, aggregate size and type, additive curing time etc., on some pavement characteristics.

The literature, however, reveals a considerable deficiency in research related to the subject of field

0022–2461

compaction, i.e. improved methods of field compaction for improved pavement performance. The traditional methods of using cylindrical steel rollers, which have limitations in both the geometry and materials, have not changed considerably for almost the past half-century. In addition, the inadequacy of providing confinement during compaction results in pavements with less uniform densities and strength, which renders the pavements vulnerable to initial cracking during construction [1]. Various workers have found that in order to overcome initial cracking problems of asphalt pavements, when using wheel rollers, the rigidities as well as the geometry of the rollers must be more compatible with the asphalt mix. Modification in geometry of the compaction system, would require a tremendous increase in diameter of the rollers to permit a flat contact surface between the compacted asphalt mix and the roller. Thus, focused research is needed to improve field compaction methods in order to improve the pavement performance and prevent premature failure. Moreover, tests developed to evaluate the various compaction methods must take into account the long term performance of the pavement, i.e. fatigue crack propagation studies.

In the present work, the effect of processing conditions (a modified Marshall hammer technique, to include dynamic compaction together with the conventional static compaction) on both the mechanical properties and the fracture toughness (resistance to fatigue crack propagation) of an AC-20 asphalt concrete mixture was studied. The objective of the current work is to demonstrate the tremendous enhancement of the fatigue resistance of the AC-20 mixture as a result of better compaction. This technique could potentially be implemented in the field, along with the equipment currently being used. Micromechanical studies using scanning electron microscopy were performed to explore the microstructural features of the dynamically and statically compacted mixture, in comparison with the conventional statically compacted mixture.

2. Fatigue crack propagation analysis

Traditionally fatigue studies on pavements have been conducted through two classic approaches. These are the phenomenological approach [4–7] and the fracture mechanics approach based on Paris type equations [8–10]. Recently, the modified crack layer (MCL) model has been introduced and applied to characterize the resistance of pavement to crack propagation [11–13]. The MCL model expresses the crack speed as:

$$\frac{da}{dN} = \frac{\beta' \dot{W}_i}{(\gamma' a - J)} \tag{1}$$

where a is the crack length and N is the number of cycles. The energy release rate, J, is given as:

$$J = \frac{(\delta P/\delta a)}{B} \tag{2}$$

where P is the potential energy (area above the unloading curve) and B is the width of the specimen. The change in work, $\dot{W}_i$, is given as:

$$\dot{W}_i = \frac{h_o - h_i}{B} \tag{3}$$

where h_i is the area of the hysteresis loop at crack length a and h_o is the area of the loop just before crack initiation. Rearranging Equation 1 gives:

$$\left(\frac{J}{a}\right) = \gamma' - \beta'\left[\frac{\dot{W}_i}{a(da/dN)}\right] \tag{4}$$

where γ' is the specific energy of damage characteristic of the material's resistance to crack propagation and β' is the energy dissipative character of the material. These parameters can be extracted from fatigue crack propagation experiments using Equation 4.

In the present work, the effect of processing conditions (dynamic and static compaction) on the fracture resistance of AC-20 asphalt concrete mixture will be studied employing the modified crack layer model.

3. Materials and specimen preparation

3.1. Aggregate type and gradation

Crushed limestone aggregate and quartizitic sand were selected for the preparation of test specimens. Gradation requirements met Ohio Department of Transportation 403 specification, shown in Table I.

3.2. Asphalt cement

AC-20 asphalt cement was used in the study with the physical properties given in Table II.

The required percentages of aggregate were mixed in one batch to produce asphalt concrete beams with a target unit weight of 2387 kg m^{-3}. All beams contained 8 wt% asphalt cement, as a percentage of the total mix. This percentage corresponds to the optimum asphalt cement content, as determined by the Marshall method of mix design. The beams were prepared in agreement with ASTM D3202-83.

TABLE I Aggregate gradation

Sieve size	Percentage of total aggregate
1/2″–3/8″	5
3/8″–#4	36
#4–#16	31
#16–#50	19
#50–#200	9
Passing #200	0

TABLE II Physical properties of AC-20 asphalt

Physical properties	AC-20
Penetration at 25 °C (ASTM D-5)	76
Viscosity at 135 °C, m^2 s^{-1} (ASTM D-2170)	0.0400
Viscosity at 60 °C, Pa s (ASTM D-2171)	196.9
Flash, (Cleveland Open Cup), °C (ASTM D-92)	315.55

3.3. Static compaction procedure

The aggregate mixes and the asphalt cement were heated to a temperature ranging between 149 and 190.5 °C, along with the compaction mould and the mixing tools. The aggregate was then blended with the required amount of asphalt cement (8% of the total weight of mix) as quickly and thoroughly as possible to yield a mixture having a uniform distribution of asphalt cement. The heated mould was then filled with the heated asphalt cement–aggregate mixture, followed by its static compaction by applying a uniform pressure of 13.79 MPa through a 50.8 × 381 mm plate with a hydraulic press for 1 min. The compacted beam was allowed to cool off in the mould before its removal, and was usually tested 7 days after preparation and curing. Curing was done by subjecting each beam to a constant temperature of 60 °C for one day. The air void content for the conventionally compacted specimens was 1.3%.

3.4. Dynamic compaction procedure

The equipment required for the dynamic/static compaction includes a modified Marshall compaction hammer having a 44.48 N weight and a 0.457 m drop. The compaction face was modified to accept a 152.4 × 50.8 mm rectangular plate, instead of the usual 98.4 mm diameter circular tamping base. The base of the compaction hammer was also preheated using a bath of boiling water as a convenient method. The heated mould placed on a compaction pedestal was filled with the heated asphalt–aggregate mix to about half of the depth of the mould, and then a total of 30 blows were applied at three locations along the length of the beam (10 blows per location). The remaining heated asphalt–aggregate mix was added to the mould as in the first stage, and another series of 30 blows were applied. Following the dynamic compaction procedure, the beam was subjected to a pressure of 206.85 kPa in a hydraulic press for 5 min. The compacted beam was then allowed to cool off in the mould before its removal, and was usually tested 7 days after preparation and curing. Curing was the same as for the conventionally compacted specimens. The air void content was about 1.24%.

Three identical specimens were tested for both AC-20 static compaction and AC-20 dynamic and static compaction. These two different processes will be named as AC-20 (NH) and AC-20 (H), respectively. The overall specimen dimensions were 381 × 50.8 × 89 mm for the no hammer beams, and 381 × 50.8 × 89 mm for the hammer specimens.

4. Laboratory testing

4.1. Static flexure tests

The asphalt concrete beams were tested under static flexure in order to determine the flexural modulus, E, the ultimate bending stress and the ultimate load for each mixture. A screw driven testing machine with a 22.24 kN load cell was used to conduct the static flexural tests on the beams subjected to symmetrical four point loading. This loading configuration produces an increasing static pure bending moment over the middle third of the 381 mm long beams. The machine is provided with an upper fixed head and a lower platen with two end supports 254 mm apart. The beam deflection is measured with an Linear Variable Differential Transformer (LVDT) and the load–deflection curve is recorded by means of an x–y plotter. After setting the beams on the supports and fitting the loading head on the top surface of the beam, the load is applied gradually at a constant rate until failure is reached.

4.2. Fatigue crack propagation tests

Four point bending fatigue crack propagation tests were performed using a repeated pneumatic flexure testing machine fitted with a 4.448 kN load cell. Tests were conducted in a laboratory environment at a constant temperature of about 21.1 °C using an invert haversine wave type of load. The load application period was 0.2 s followed by a 2 s rest period between repeated loads. As in the static flexural test, the support span was equal to 254 mm, and the midspan loading points were separated by 84.7 mm. A straight notch in the middle of the specimens was inserted to a 6.35 mm depth with a 4 mm saw, with a round tip of radius 2.4 mm. A maximum load of 289.1 N was used, with continuous cycle load applications from zero to the maximum load. A hysteresis loop (load versus deformation) was recorded at 6.35 mm intervals of crack growth using the x–y plotter. Software was developed to digitize graphical data and to calculate pertinent areas within the load–deflection curves obtained during fatigue testing.

5. Results and discussion

5.1. Flexural fracture behaviour

Relationships between the load and deflection for dynamically and statically compacted AC-20 (H) specimens, as well as the statically compacted specimens AC-20 (NH), are shown in Fig. 1. It is noticed that for mixtures where dynamic compaction was used, the flexural modulus was two times higher and the ultimate strength increased by about 2.5 times, as compared to the mixture where static compaction alone was used. It is also to be noticed that the area under the load–deflection curve increased significantly for the dynamic compaction mixture, giving an indication that the mixture's toughness has also increased. Results of flexural testing are shown in Table III.

5.2. Fatigue crack propagation analysis

Relationships between the crack length, a, and the number of cycles, N, for each mixture are shown in Fig. 2. Cracking initiated at about 1800 cycles and advanced very rapidly, reaching its fatigue life at about 2500 cycles in the statically compacted AC-20 (NH) specimen. Crack initiation in the dynamically and statically compacted AC-20 (H) mixture, started at 8000 cycles and then advanced at a slower rate than in the statically compacted mixture, reaching its fatigue life at about 14 000 cycles. Thus, the fatigue life of

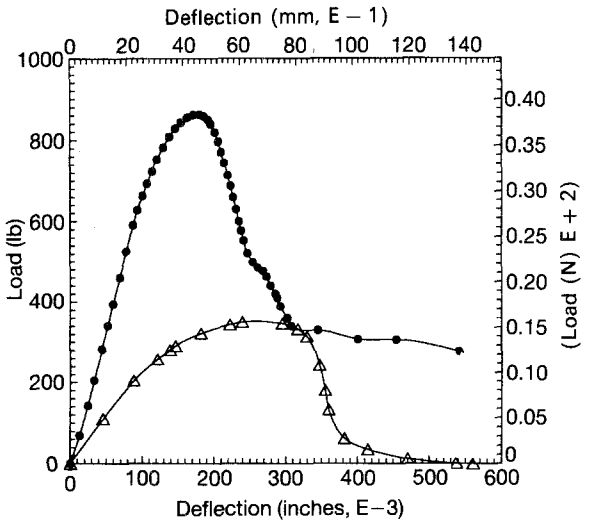

Figure 1 Load versus load point displacement of the (●) AC-20 dynamically/statically (H) and (△) statically (NH) compacted asphalt concrete mixtures.

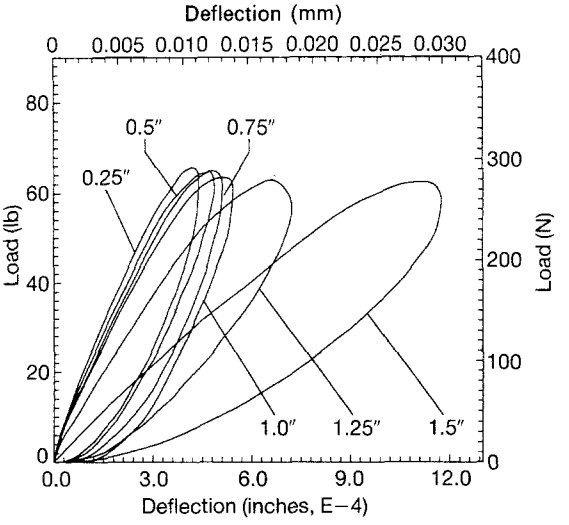

Figure 3 Hysteresis loops recorded at intervals of crack length for the dynamically/statically compacted (AC-20 hammer) mixture.

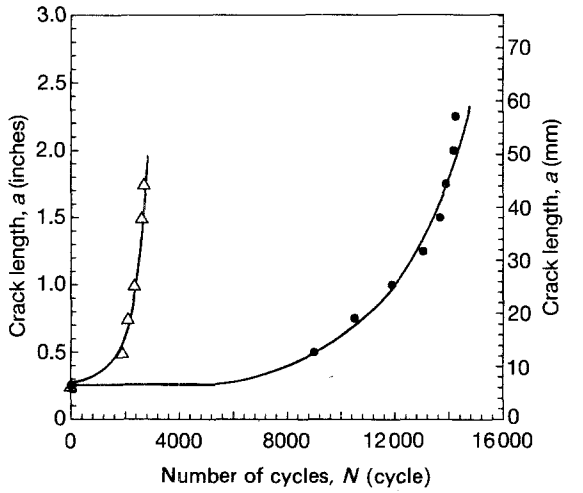

Figure 2 Crack length, a, versus number of cycles, N, for the (●) dynamically/statically (H) and (△) statically (NH) compacted AC-20 asphalt concrete mixtures.

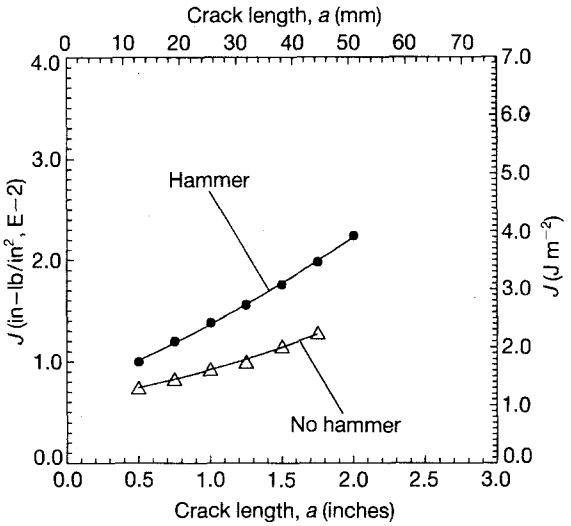

Figure 4 Energy release rate, J, versus crack length, a, for the (●) dynamically/statically (hammer) and (△) statically (no hammer) compacted AC-20 asphalt concrete mixtures.

TABLE III Mechanical properties of AC-20 mixtures

Mixture	Ultimate load (N)	E (MPa)	Ultimate bending strength (MPa)
AC-20 Dyn/Stat	3825.3	73.8	2.420
AC-20 Stat	1556.8	37.2	0.985

the dynamically and statically compacted AC-20 (H) specimens increased by about 5.6 times as compared to the life of the statically compacted AC-20 (NH) specimens. Also, the number of cycles for crack propagation (number of cycles after crack initiation) for the dynamically and statically compacted AC-20 (H) mixture is higher by about 8.5 times, as compared to that of the statically compacted mixture; which also indicates that the mixture's resistance to crack propagation has been considerably increased by using the dynamic compaction procedure. The slope of the curves in Fig. 2 is the average crack speed, da/dN, at a given crack length, a.

Typical hysteresis loops generated at intervals of crack length for the AC-20 hammer mixture are shown in Fig. 3. The area above the unloading curve for both mixtures at various crack lengths was plotted as a function of crack length. The first derivative of this curve, at various crack lengths divided by the specimen thickness, is the energy release rate, J, at the corresponding crack length.

Values of the energy release rate, J, are calculated and plotted versus the crack length, a, for each mixture and are shown in Fig. 4, indicating that the energy release rate is always higher in the case of the dynamically and statically compacted (H) mixtures, as compared to that of the statically compacted (NH) mixtures for the same crack length. This can be attributed to the fact that the AC-20 (H) mixture requires more energy to overcome the interfacial adhesion between the binder and the aggregate and the cohesion of the binder which has been enhanced by better compaction. Values of J will be used in Equation 4 to evaluate γ' and β' for each mixture.

In a stress controlled flexural test, the area of the hysteresis loop, h_i, at intervals of crack length, a, can be calculated and plotted against the corresponding crack length. By considering the value of the area of the hysteresis loop just before the crack initiation as a reference, h_o, the values of the irreversible work, $\dot{W}_i$, are obtained from Equation 3 for each mixture at different crack lengths. These are then used in Equation 4.

In order to evaluate the parameters γ' and β', which characterize the resistance of the two asphalt concrete mixtures to fatigue crack propagation, Equation 4 is employed. A plot of J/A versus the terms between the brackets in Equation 4 should give a straight line if the data are in accord with the theory. It is observed that all points nearly plot along a straight line, Fig. 5, from which γ' (the intercept) and β' (the slope) can be extracted. The average values of γ' and β' for each mixture are shown in Table IV. It is observed from Table IV that the average value of γ' for the dynamically and statically compacted AC-20 (H) mixture is about 1.8 times higher than that for the statically compacted AC-20 (NH) mixture; while the value of β' for the statically compacted AC-20 mixture is about 13 times higher than the value for the dynamically and statically compacted AC-20 (H) mixture. A larger value of γ' indicates that more energy is required to cause a unit volume to change from undamaged to damaged material, while a higher value of β' reflects the larger percentage of energy expended on dissipative processes and damage growth within the active zone. These two observations indicate that the dynamically and statically compacted AC-20 (H) mixture is more resistant to crack propagation than the statically compacted AC-20 (NH) one.

Plots of da/dN versus the energy release rate, J, for the two asphalt concrete mixtures under consideration, display the familiar S-shape, as shown in Fig. 6. As it can be seen in Fig. 6, particularly for the hammer behaviour, three stages of crack propagation are obvious. The initial threshold stage is followed by a stage of reduced acceleration as the crack length increases, followed by a stage of critical crack propagation. The fatigue crack propagation curve is approximately linear in the second region, while in the third region the rate of fatigue crack propagation approaches its asymptotic value where transition from stable to unstable conditions occurs. It is also obvious from Fig. 6, that the hammer mixture displays a superior fatigue crack propagation resistance than its counterpart.

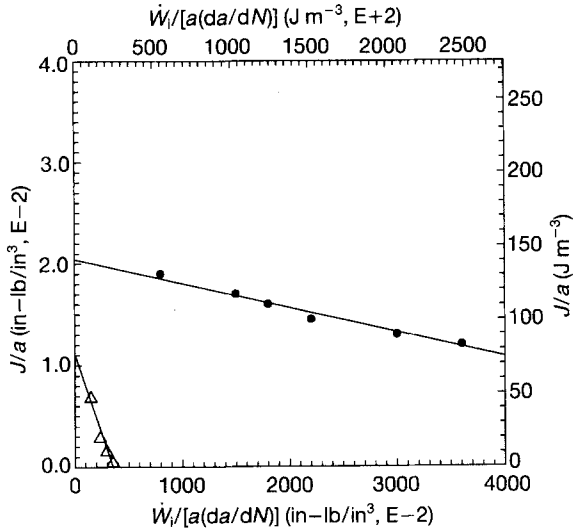

Figure 5 Fatigue crack propagation behaviour of (●) the dynamically/statically (H) and (△) statically (NH) compacted AC-20 asphalt concrete mixtures, plotted in the form of the MCL model to obtain γ' and β'.

TABLE IV γ' and β' for AC-20 mixtures

Mixture	γ' (J m^{-3})	β'
AC-20 Dyn/Stat	141 ± 20	$2.40 \pm 0.15 \times 10^{-4}$
AC-20 Stat	77 ± 15	$3.14 \pm 0.20 \times 10^{-3}$

5.3. Microscopy

Visual observation and global (× 12) scanning electron microscopic (SEM) examination have revealed that dynamic compaction combined with static compaction has created a finer more dense texture. Deep large size voids and gaps are seen between the aggregate particles for the statically compacted mixture. These voids appear to be smaller and the fracture surface morphology appears finer for the dynamically and statically compacted mixture. At higher magnification (× 100) focus is placed on a binder rich area of each mixture. Large dimples can be seen in Fig. 7, on the fracture surface of the statically compacted AC-20 mixture. On the other hand, more dimples per unit area, Fig. 8, are associated with the dynamically and statically compacted AC-20 mixture. Again, this illustrates the dense nature of the packing, which increases the surface area of contact between the aggregate and binder. It is believed that this is the mechanism by which the dynamically and statically compacted AC-20 mixture earns its superior fracture resistance. Higher magnification (× 2000), which focuses on the

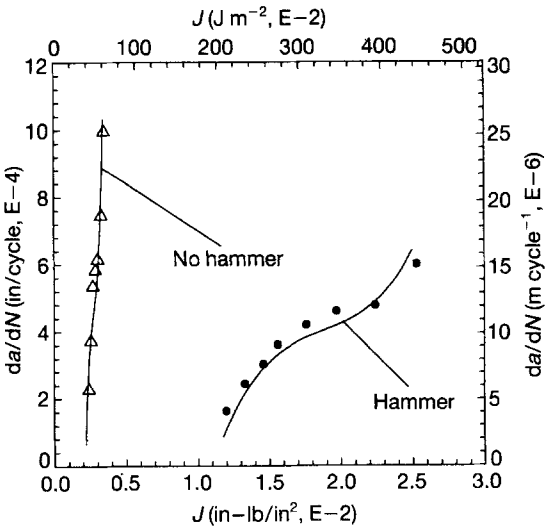

Figure 6 The theoretically predicted fatigue crack propagation speed based on the MCL model (together with the experimental data) for (●) the dynamically/statically (hammer) and (△) statically (no hammer) compacted AC-20 asphalt concrete mixtures.

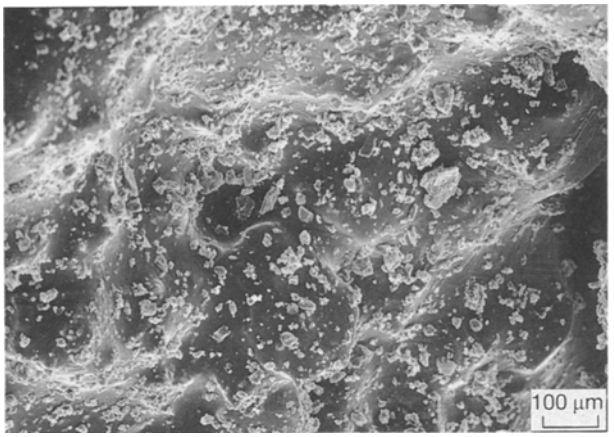

Figure 7 Microstructural features of the AC-20 statically compacted (no hammer) mixture at ×100 magnification.

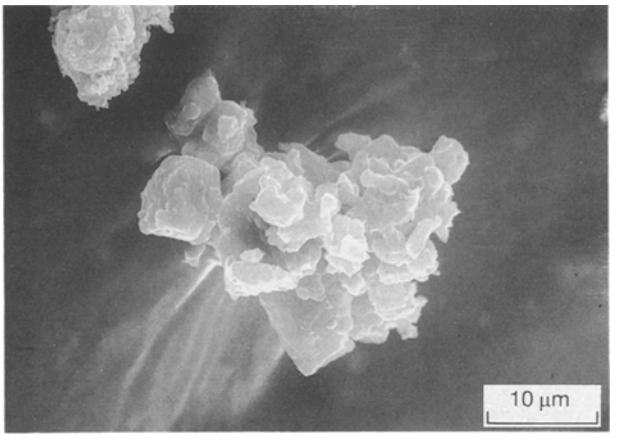

Figure 9 The morphology of fine aggregate particles in the statically compacted (no hammer) mixture at ×2000 magnification.

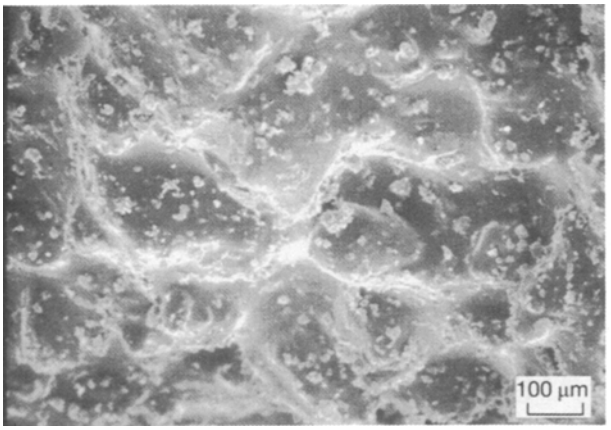

Figure 8 Microstructural features of the AC-20 dynamically/statically compacted (hammer) mixture at ×100 magnification.

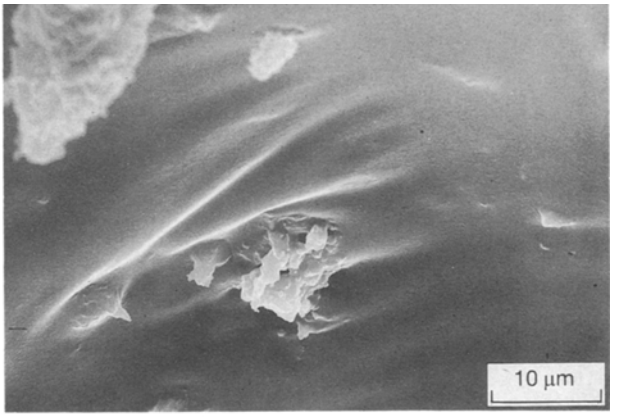

Figure 10 The morphology of fine aggregate particles in the dynamically/statically compacted (hammer) mixture at ×2000 magnification.

fine aggregate particles present in both mixtures, Figs 9 and 10, for the statically and dynamically compacted specimens, reveals that the fine particles are better coated with more fine ridges surrounding them for the dynamically and statically compacted AC-20 mixture, Fig. 10. Again, this attests to the better adhesion of the binder to the aggregate.

6. Conclusions

Laboratory induced compaction, employing a modified Marshall hammer technique, has increased both the ultimate strength and the flexural modulus of AC-20 mixture by about two-fold. Considerable enhancement of the fracture resistance of the AC-20 mixture was achieved by modifying the Marshall hammer to include dynamic compaction. The modified crack layer (MCL) model successfully characterized the resistance of the statically and the dynamically/-statically compacted AC-20 specimens over the entire range of their energy release rate. A higher value of γ' and lower value of β' is associated with the AC-20 mixture prepared with the dynamic and static compaction method. This attests to the fracture resistance superiority of this mixture.

Microscopic analysis has revealed differences in the macro- and microstructure of the dynamically/statically compacted AC-20 mixtures. Evidence of smaller, more frequent dimples, indicative of more surface contact between the aggregate and binder have been observed. It is believed that these are the mechanisms by which the dynamically/statically compacted AC-20 acquires its toughness.

Acknowledgements

This work has been sponsored by the Army Corps of Engineers, Waterways Experiment Station, Vicksburg, MS, USA. The direction of Drs N. Brabston, L. Lewandowski and R. Rollings, of the Army Corps of Engineers is also gratefully appreciated.

References

1. A. O. ABD EL-HALIM and O. SVEC, in Proceedings of Canadian Technologists Asphalt Association, Vol. 35, 1990, (Polyscience Pub. Inc., Quebec, Canada) pp. 18–33.
2. J. KINDBERG, *ibid.* Vol. 35, 1990, pp. 276–286.
3. A. CONSUEGRA, D. N. LITTLE, H. VON QUINTUS and J. BURATI, Transportation research record 1228, Transportation Research Board, National Research Council, Washington, DC (1989) pp. 80–87.
4. C. L. MONISMITH, K. E. SECOR and E. W. BLACKMER, in Proceedings of the Association of Asphalt Paving Technologists, Vol. 30, 1961, (Charlston, SC) p. 188–222.

5. C. L. MONISMITH, "Asphalt mixture behavior in repeated flexure", Report No. TE 64-2, University of California, Berkeley.
6. P. S. PELL, in Proceedings of the First International Conference on the Structural Design of Asphalt Pavements, 1962 (University of Michigan, Ann Arbor, MI) p. 310.
7. P. S. PELL and I. F. TAYLOR, in Proceedings of the Association of Paving Technologists, 1969, Vol. 37, Los Angeles, CA, pp. 423–458.
8. K. MAJIDZADEH, E. KAUFFMANN and C. SARAF, in ASTM STP 508, American Society for Testing and Materials, Philadelphia, PA, 1972, pp. 67–83.
9. K. MAJIDZADEH and D. RAMSAMOOJ, "Applications of fracture mechanics for improved design of bituminous concrete", FHWA Report, FHWA-RD-76-91, June 1976, Federal Highway Administration.
10. P. F. GERMANN and R. L. LYTTON, "Methodology for predicting the reflection cracking life of asphalt concrete overlays", Report No. TT-2-8-75-207-5, Texas Transportation Institute, College Station Texas, 1979.
11. H. AGLAN, *Int. J. of Damage Mech.* **2** (1993) 53.
12. H. AGLAN, I. SHEHATA, L. FIGUEROA and A. OTHMAN, "Structure–fracture toughness relationship of asphalt concrete mixtures", Transportation Research Record No. 1353, (Transportation Research Board, National Research Council, Washington DC, 1992) pp. 24–30.
13. H. AGLAN and L. FIGUEROA, *J. Eng. Mech.* **119** (1993) 1243–1259.

Received 6 May
and accepted 18 August 1993